

Monte Carlo Simulation of the Phase Diagram of C₆₀ Using Two Interaction Potentials. Enthalpies of Sublimation

Rui P. S. Fartaria, Fernando M. S. Silva Fernandes,* and Filomena F. M. Freitas

Laboratory of Molecular Simulation and CECUL, Department of Chemistry and Biochemistry, Faculty of Science, University of Lisboa, Rua Ernesto de Vasconcelos, Bloco C8, Piso 3, 1749-016 Lisboa, Portugal

Received: May 23, 2002; In Final Form: July 26, 2002

A first-principles interaction potential proposed by Pacheco and Ramalho (PRP) and the effective potential of Girifalco (GP) have been used to model the whole phase diagram of C₆₀ by Gibbs ensemble and Gibbs–Duhem integration Monte Carlo methods. The triple-point properties were determined by a direct method recently proposed by us (*Comput. Phys. Commun.* **2001**, *141*, 403). It is based on the behavior of the Gibbs ensemble vapor–liquid simulations at the low-temperature limit, and it does not involve free-energy calculations. A stable liquid phase for temperatures between 1570 ± 20 K and 2006 ± 27 K is predicted with the PRP model and for temperatures between 1529 ± 36 K and 1951 ± 28 K with the GP model. According to these results, the liquid phase for C₆₀ extends over ~ 450 K, a temperature range considerably wider than the ones reported by other authors on the basis of free-energy calculations and density functional approaches. Nonetheless, the present results are in good agreement with the theoretical predictions from the hypernetted mean spherical approximation, the modified hypernetted chain theory, and a correlative self-consistent field method as well as with some molecular dynamics simulations. The reported free-energy data for the fluid–solid region are reproduced here, strictly by computer simulation. According to them, the liquid phase of C₆₀ extends over ~ 100 K. A discussion on the apparent conflicting triple-point data is presented. The calculated enthalpies of sublimation at 700 K (163 ± 9 kJ mol^{−1} for PRP and 170 ± 12 kJ mol^{−1} for GP) are in good agreement with the available experimental results. The estimated standard enthalpies are also within the recommended values, and the third-law enthalpies are in excellent agreement with experimental and theoretical data. This suggests that at least the simulated triple-point properties, in the low-temperature limit, should approach that of real C₆₀. The radial distribution functions and the self-diffusion coefficients, in the liquid pockets predicted for the two models, are also consistent with a normal liquid state, and no sign of liquid supercooling was observed. On the whole, the differences between the present interaction potentials do not induce significant qualitative changes in the phase behavior of the two models. However, the differences are clearly reflected in the location of the coexistence lines and the critical and triple-point properties as well as in the enthalpies of sublimation. Finally, as a further test of the reliability of our method for the determination of triple-point properties, we also report preliminary results for the triple-point temperature and the standard enthalpy of sublimation of C₇₀. They are in excellent agreement with theoretical and experimental data.

1. Introduction

Recently, we have reported the vapor–liquid and fluid–solid coexistence properties of a C₆₀ model¹ using a first-principles interaction potential (PRP) proposed by Pacheco and Ramalho.² The pioneering works of Hagen et al.³ and Cheng et al.⁴ in 1993, based on an effective potential (GP) proposed by Girifalco,⁵ gave rise to a controversial question of the existence of a stable liquid phase for C₆₀. The first group, using a combination of simulation and free-energy methods, concluded that C₆₀ does not have a stable liquid phase because the sublimation line was located 35 K above the critical temperature at 1798 K. The second group used the hypernetted mean spherical approximation (HMSA) combined with molecular dynamics to predict a stable liquid phase between 1774 and 1900–2050 K.

Since then, part of the simulation and free-energy calculations,^{6–10} as well as some density functional approaches,^{11–13} presented two types of behavior. Either no triple point was predicted or a triple point was estimated, but a liquid phase remained below it. If the liquid there is metastable, then no conflict with thermodynamics exists. However, the extensive

Gibbs ensemble vapor–liquid simulations of Caccamo et al.¹⁴ suggest that the liquid phase is stable below the triple points estimated from the free-energy-based calculations. Moreover, the theoretical studies based on the hypernetted mean spherical approximation (HMSA)⁴, the modified hypernetted chained theory (MHNC),^{15,16} and a correlative self-consistent method¹⁷ as well as some molecular dynamics simulations¹⁸ point to the existence of lower triple-point temperatures than the ones from free-energy studies. Such behaviors were the object of our work referred to above in which it was demonstrated, strictly by computer simulation, that a model of C₆₀ is able to reproduce two sets of apparently conflicting triple-point properties: one, in the high-temperature limit, according to the free-energy results and the other, in the low-temperature limit, according to the findings of HMSA and MHNC theories.

Our simulations were carried out by the Gibbs ensemble Monte Carlo (GEMC)^{19,20} and the Gibbs–Duhem integration Monte Carlo (GDIMC)²¹ methods. Furthermore, we have proposed²² a new approach to estimate the location of the triple point. The method is based on the limiting behavior of the Gibbs ensemble vapor–liquid calculations for the lowest temperature range. It provides, in a direct and natural way, a starting state (the triple point) for the simulation of the fluid–solid coexist-

* Corresponding author. E-mail: fsilva@fc.ul.pt.

ence by GDMC. Also, it constitutes an alternative to the perturbation technique proposed by Agrawal and Kofke^{23,24} to circumvent one of the limitations of the Gibbs–Duhem scheme to trace coexistence curves.

In this work, we present results from GEMC and GDMC simulations of the whole phase diagram of C₆₀ using PRP and GP. Indeed, most of the simulations carried out hitherto have used these interaction models. The main objectives of the present article are (i) to extend our previous work to the vapor–solid coexistence properties of C₆₀; (ii) to assess the effect of the differences between the interaction potentials on the phase behavior; and (iii) to compare the respective enthalpies of sublimation with the available experimental results. We also reaffirm that it is possible to estimate, strictly by computer simulation, conventional triple points for the two models in accordance with some theoretical predictions and the basic concepts of thermodynamics.

Whether or not the present simulation results correspond to the whole phase diagram of real C₆₀ is a matter that can be settled only with further experimental and theoretical investigation. In fact, molecular dynamics simulations^{25,26} predict that an isolated C₆₀ molecule is stable up to ~4500 K. However, some experiments^{14,9,27} show that C₆₀ molecules in the solid phase are unstable against polymerization or amorphization well below the temperatures of interest (~2000 K). Nevertheless, we believe that the present work sheds light on the main aspects of the present potential models for C₆₀ and that it may be useful in the experimental field. In fact, we shall see that the simulated enthalpies of sublimation are in good agreement with the available experimental data, suggesting that at least the triple-point properties, in the low-temperature limit, should approach those of real C₆₀. Moreover, those properties seem to be consistent with a kind of “corresponding state” rule for fullerenes recently reported by Abramo et al.²⁷

In the next section, we present the potential models and computational details. The results are shown and discussed in sections 3 and 4. The final section contains the conclusions of this work.

2. Potential Models and Computational Details

The ab initio PRP² is composed of a short-range term,

$$M(r) = M_0 \exp\left[\tau\left(1 - \frac{r}{d_0}\right)\right] \left\{ \exp\left[\tau\left(1 - \frac{r}{d_0}\right)\right] - 2 \right\} \quad (1)$$

a long-range term,

$$W(r) = -\frac{C_6}{r^6} - \frac{C_8}{r^8} - \frac{C_{10}}{r^{10}} - \frac{C_{12}}{r^{12}} \quad (2)$$

and a Fermi-type crossover function,

$$F(r) = \left\{ 1 + \exp\left[\frac{r - \mu}{\delta}\right] \right\}^{-1} \quad (3)$$

The final form of the potential is

$$V(r) = F(r) \times M(r) + [1 - F(r)] \times W(r) \quad (4)$$

with the parameters given in the original article. GP⁵ has the form

$$V(r) = -\alpha \left[\frac{1}{s(s-1)^3} + \frac{1}{s(s+1)^3} - \frac{2}{s^4} \right] + \beta \left[\frac{1}{s(s-1)^9} + \frac{1}{s(s+1)^9} - \frac{2}{s^{10}} \right] \quad (5)$$

with the parameters given in the original articles.

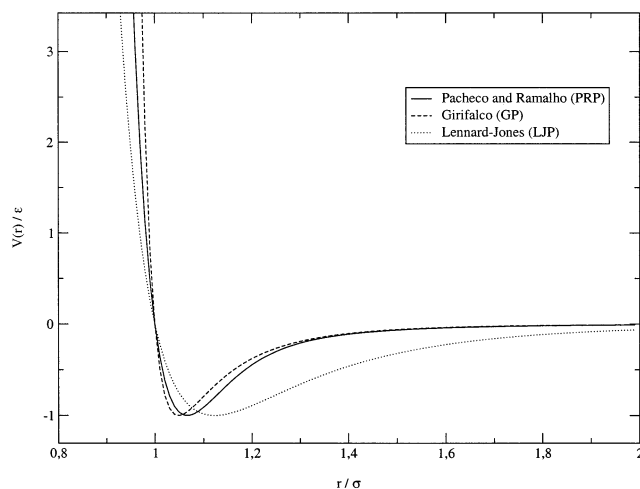


Figure 1. Comparison of PRP and GP with LJP (ϵ is the well depth, and σ is the effective molecular diameter).

PRP is softer than GP, but they both are significantly harder and narrower and decay much more rapidly to zero than the Lennard-Jones potential (LJP), as can be seen in Figure 1. These aspects could be the origins of the apparent anomalous behavior detected in the fluid–solid region of C₆₀ when compared with the well-behaved trend observed in the diagram of the LJ system. Either PRP or GP seem to be, at least as a first step, appropriate to model C₆₀. However, PRP reproduces the experimental pressure–volume isotherm at high pressures more accurately than GP.²

Although PRP is a first-principles accurate potential, it depicts (as GP does) $V(r)$ for an r measured from the center of the approximately spherical C₆₀ molecule. This may mask the true nature of the interactions responsible for the convexity properties of the free energy. Indeed, they may arise from a more cooperative interaction of clusters. Ashcroft,²⁸ for example, touches upon the problem in an interesting note commenting on the results of Hagen et al.³ and Cheng et al.⁴ That is a serious suggestion not taken into account in the present study.

The rationale for essentially noble gas models is, above all, the use of the simplest and most plausible ab initio and effective potentials to probe the phase behavior of C₆₀. This may well turn out, however, to be a crude approximation, at least for some regions of the phase diagram.

The potentials were truncated at half of the simulation box lengths. This distance was always larger than 2σ (σ is the effective diameter of the molecule). Long-range corrections (LRC) were not included because the potentials rapidly decay to zero for distances greater than 2σ . Nonetheless, taking into account the study of Hasegawa and Ohno,¹³ we have verified that the truncation distances that were used have negligible effects on the phase behavior. For distances smaller than 0.3σ , the potentials were switched to ∞ because at these values of proximity the potential energy is very high and the configurations would always be rejected. Also, for separations smaller than 0.2σ , PRP reaches high negative values, and any configuration would be accepted. The usual cubic periodic boundary conditions were always applied.

The vapor–liquid coexistence curves were obtained by GEMC simulations. The first point was set up by placing the molecules in face-centered cubic (fcc) lattices with 256 molecules in each box, at appropriate densities, and running the convenient number of cycles for a complete relaxation of the system. The other points were calculated starting from fcc lattices with 256 molecules in each box, at the equilibrium densities of the previous runs. Equilibration runs of 3000–10 000 cycles were followed by production runs of 20 000–

40 000 cycles. A GEMC cycle consisted of random displacements of each molecule, a random rearrangement of the volume of each box (keeping the total volume constant), and a number of trials to transfer a molecule from one box to another, with a rate of acceptance of $\sim 1\%$ of the total number of trials.

The liquid–solid and vapor–solid coexistence curves were calculated by the GDMC method. It consisted of successive and simultaneous NpT simulations in two boxes (each containing 256 molecules) combined with a predictor–corrector scheme to estimate the temperature, as a function of pressure, for the next point along the coexistence line. The coupling procedure described by Kofke²¹ was applied in some calculations.

An important issue in fluid–solid simulations by the GDMC method is the definition of the starting state to initiate the integration of the Clapeyron equation. In the present study, two methods were applied. The first one is an adaptation of Agrawal and Kofke's method.^{23,24} From the known properties of the soft-sphere potential (SSP), in the limit of high-temperature, we determined the starting phase points through the scaled potential

$$V(r, \lambda) = (1 - \lambda) \text{SSP}(r) + \lambda V(r) \quad (6)$$

where λ is a parameter between 0 and 1 and $V(r)$ is the potential of interest. From that point, we calculated the other points at lower temperatures.

The second method is the one proposed by us. The full computational details of the method can be seen in the original article.²² In short, it consists of decreasing the temperature of the GEMC vapor–liquid equilibrium by small steps ($\Delta T \approx 10$ K) until a temperature is reached below which the liquid phase is not stable anymore. The system readily assumes a vapor–solid configuration, that is to say, spontaneous freezing is detected in the high-density box. Those values of the temperature, the densities and configurational energies (just before and after freezing), and the vapor pressure are taken as an estimation of the triple-point properties. From that point, in the low-temperature limit, we successively calculated the fluid–solid lines by increasing the temperature and the vapor–solid lines by decreasing the temperature.

It may be argued that this method does not have the reliability that would warrant anything more than a qualitative conclusion regarding the true freezing temperature. We should mention, however, that in the original article²² ample evidence was given of the quantitative correctness of the method. In particular, it was demonstrated that the method does not lead to the supercooling of the liquid if the conditions of the respective computational algorithm are fulfilled. Furthermore, it is able to determine the triple-point temperature in a very narrow interval (± 10 K for C₆₀) within the maximum error usually reported for that property. The results obtained by the two methods are significantly different, as we shall see in the following section.

3. Phase Diagrams

The whole temperature–density phase diagram of C₆₀ obtained from the two potential models is presented in Figure 2. The fluid–solid and vapor–solid coexistence lines were obtained from the starting state defined by our method.

Figure 3 displays part of the diagram with the fluid–solid coexistence lines calculated from the starting state defined by Agrawal and Kofke's method.¹ It is important to include them here regarding the discussion ahead.

Table 1 displays some critical- and triple-point properties obtained by various authors for PRP and GP. The critical temperatures and densities were estimated by fitting the vapor–liquid data to the laws of rectilinear diameters and order-parameter scaling²⁹ with a critical exponent of ~ 0.33 . The

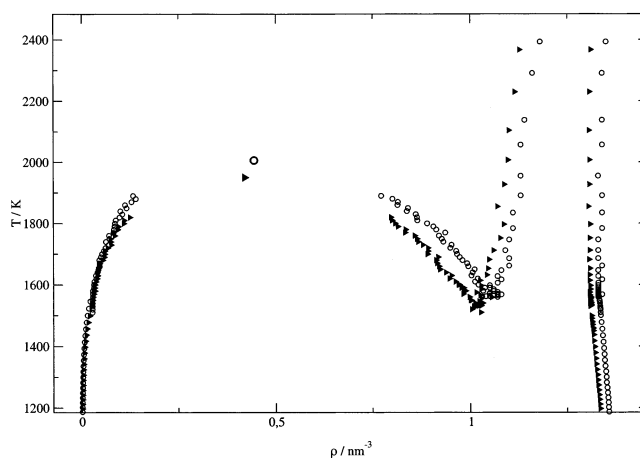


Figure 2. Temperature–density phase diagram: (○) PRP, (▲) GP (the fluid–solid and vapor–solid lines were obtained from the starting state defined by our method^{1,22}).

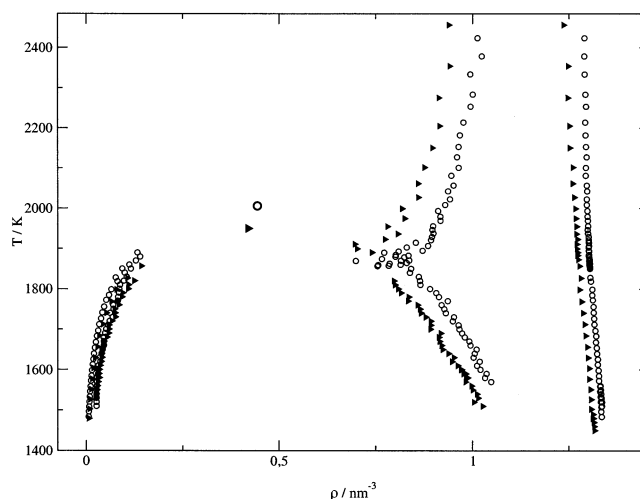


Figure 3. Part of the temperature–density phase diagram: (○) PRP, (▲) GP (the fluid–solid lines were obtained from the starting state defined by Agrawal and Kofke's method^{23,24}).

pressures were fitted to the Clapeyron equation. The final triple-point properties were assessed by fitting the fluid–solid raw data and intersecting the extension of the vapor–liquid lines with the freezing lines. The pressure–temperature diagrams are displayed in Figure 4.

The vapor–liquid curves show the usual behavior (see Figure 2). As expected, the order parameter ($\rho_L - \rho_V$) for PRP is greater than the one for GP, giving rise to a higher critical temperature and density: 2006 ± 27 K, 0.444 ± 0.003 nm^{−3} for PRP and 1951 ± 28 K, 0.423 ± 0.003 nm^{−3} for GP. This clearly reflects the softer nature of PRP. These values compare well with the data of Ferreira et al.⁸ for PRP and that of Caccamo et al.¹⁴ and Hasegawa and Ohno⁹ for GP.

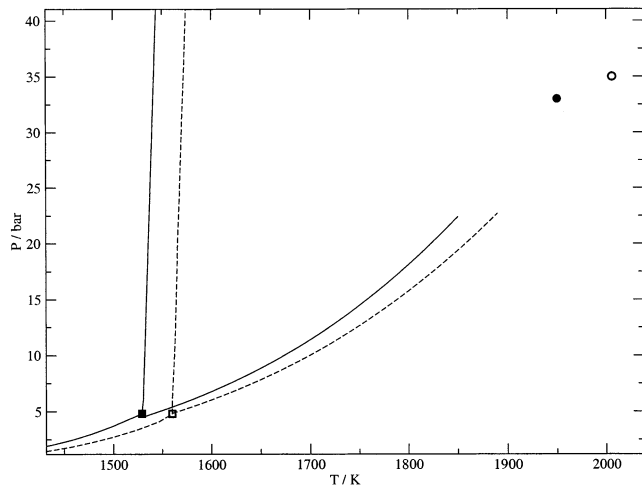
Regarding the discussion ahead, it is very important to point out that the vapor–liquid properties were checked against thermodynamic stability. This was done by confirming the equality of the chemical potentials and pressures at all the simulated points of the coexistence curves. Additionally, the analysis of the probability plots, recommended by Frenkel and Smit,³⁰ was also carried out.

The fluid–solid curves obtained with PRP are located in a higher density region than the ones from GP (see Figure 2). This also seems to reflect the softer nature of PRP. The estimated triple-point temperatures and liquid densities are 1570 ± 20 K, 1.05 ± 0.01 nm^{−3} for PRP and 1529 ± 36 K, 1.02 ± 0.01 nm^{−3} for GP. The values for GP are in excellent agreement with the

TABLE 1: Estimates of Critical- and Triple-Point Properties for PRP and GP^a

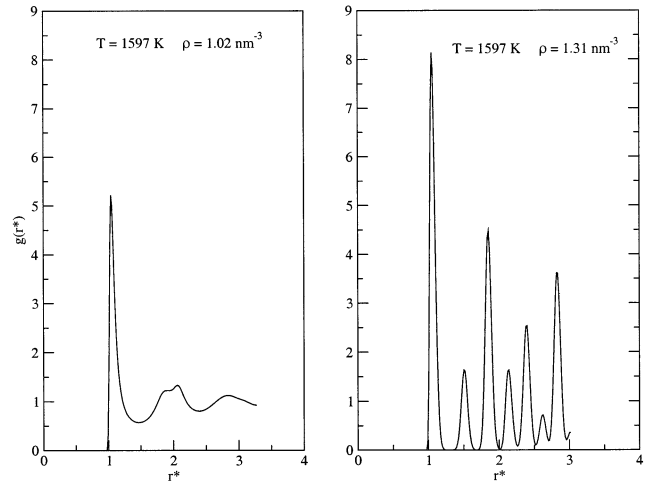
	ref	T_c/K	ρ_c/nm^{-3}	p_c/bar
PRP	1	2006 ± 27	0.444 ± 0.003	35 ± 6
	8	2011.7 ± 1.1	0.4676 ± 0.0007	
GP	this work	1951 ± 28	0.423 ± 0.003	33 ± 9
	3	1798 ± 10	~ 0.41	
	4	1900–2050	0.56	
	15	1920	~ 0.60	
	9	1980	0.44	
	14	1924–1941	0.39–0.42	29
	ref	T_{tr}/K	ρ_{tr}/nm^{-3}	p_{tr}/bar
PRP	1	1570 ± 20	1.05 ± 0.01	5 ± 16
	1	1858 ± 32	0.81 ± 0.01	19 ± 10
	8	1881.2 ± 0.1	0.8447 ± 0.0003	
GP	this work (FFF)	1529 ± 36	1.02 ± 0.01	4 ± 19
	this work (AK)	1898 ± 21	0.69 ± 0.01	26 ± 3
	4	1540	1.097	
		1774	0.944	14
	15	1620	1.0	~ 5
	9	1880	0.74	
	14	~ 1700	~ 0.91	
		~ 1500	~ 1.0	
	17	~ 1460		~ 1

^a AK means Agrawal and Kofke's method;²⁴ FFF means our method.²²

**Figure 4.** Pressure–temperature phase diagram: (– – –) PRP (□) triple point, (○) critical point); (—) GP (■) triple point, (●) critical point).

data of Caccamo et al.¹⁴ obtained by a combination of simulation and theory. It is also worth mentioning that in a theoretical study based on a correlative self-consistent field method, Zubov et al.¹⁷ estimated the triple-point temperature at ~ 1460 K from GP.

The results obtained using the method of Agrawal and Kofke^{23,24} are, however, significantly different (see Figure 3). Thus, our estimated triple-point temperatures and liquid densities by that method are 1858 ± 32 K, $0.81 \pm 0.01 \text{ nm}^{-3}$ for PRP and 1898 ± 21 K, $0.69 \pm 0.01 \text{ nm}^{-3}$ for GP. They also agree with the data of Ferreira et al.⁸ and Hasegawa and Ohno⁹ obtained by a combination of simulation and free-energy calculations. Below those points, though, a stable liquid phase is observed (see Figure 3). As referred to above, we have checked the thermodynamic stability along the vapor–liquid coexistence curves. On the basis of the values of the fluid–solid relative chemical potentials for PRP, we suggested¹ that this behavior corresponds to metastable states in the fluid–solid region. Table 2 shows the fluid–solid relative chemical

**Figure 5.** Radial distribution functions for the liquid–solid coexistence at 1597 K (near the triple point) with GP.**TABLE 2: Relative Chemical Potentials for Fluid–Solid Coexistence from GDMC with GP by Two Different Paths**

T/K	GD (AK)		T/K	GD (FFF)	
	fluid $\Delta(\beta\mu)$	solid $\Delta(\beta\mu)$		fluid $\Delta(\beta\mu)$	solid $\Delta(\beta\mu)$
2353	0.00	0.00	2374	0.00	0.00
2275	−0.57	−0.56	2105	−2.50	−2.50
2205	−1.09	−1.07	1924	−4.62	−4.60
2150	−1.53	−1.50	1798	−6.31	−6.27
2101	−1.92	−1.89	1712	−7.58	−7.53
2061	−2.25	−2.22	1653	−8.52	−8.47
2027	−2.54	−2.51	1613	−9.20	−9.14
1999	−2.79	−2.75	1585	−9.69	−9.61
1974	−3.00	−2.96	1566	−10.02	−9.95
1954	−3.18	−3.14	1554	−10.25	−10.17
1936	−3.34	−3.29	1545	−10.40	−10.32
1923	−3.46	−3.41	1539	−10.51	−10.43
1911	−3.57	−3.52	1535	−10.58	−10.50
1899	−3.67	−3.62	1530	−10.68	−10.60

potentials, $\Delta(\beta\mu)$, for GP obtained by Agrawal and Kofke's method “GD(AK)” and by our method “GD(FFF)”. The respective values for PRP and the calculation details were already reported.¹ No errors bars were determined. Even so, the coincidence of the relative chemical potentials for the fluid and solid within each set of simulations is remarkable, indicating that both calculations are consistent.

The results for GP confirm the same behavior as detected for PRP. It seems that the GD(AK) calculations were constrained to a metastable fluid–solid region of phase space. In fact, the relative chemical potentials along the two sets of fluid–solid lines show a hint of local minima for the Gibbs free energy.

As far as structural properties are concerned, we have noted the presence of shoulders in the second peak of the liquid and fluid radial distribution functions for the PRP model.¹ They were also reported by Cheng et al.⁴ from molecular dynamics of GP. We confirm the existence of these shoulders for GP in Figure 5. They indicate the presence of solid or glasslike features. This may be an interesting point regarding the suggestion of a more cooperative interaction of clusters in C₆₀ referred to above.

Radial distribution functions at different points inside the liquid pockets, determined from the low-temperature limit, were also calculated and show patterns typical of the liquid state. Additionally, we have performed canonical molecular dynamics simulations in the regions of the low-temperature triple points with 256, 864, and 2048 molecules. The self-diffusion coefficients were always on the order of $10^{-5} \text{ cm}^2 \text{ s}^{-1}$, an order of magnitude that is consistent with a normal liquid phase.^{18,27} No

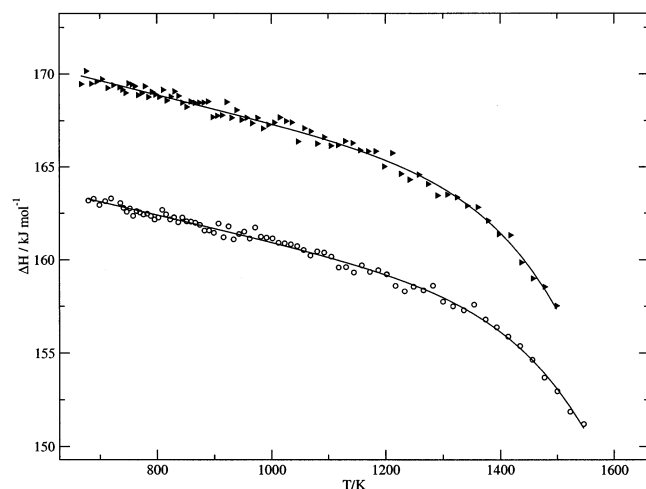


Figure 6. Enthalpies of sublimation as a function of temperature: (○) PRP, (▲) GP, (—) fitting to eq 7.

sign of liquid supercooling was observed. Finally, it is worth mentioning that the solid generated by the spontaneous freezing, detected in our method, is a quasi-perfect, not defect-rich, face-centered-cubic lattice.²²

4. Enthalpies of Sublimation and Prediction of Enthalpies of Vaporization and Melting

From the vapor–solid coexistence calculations, we worked out the enthalpies of sublimation as a function of temperature for the two models. They are displayed in Figure 6. The simulation results were fitted to the equation³¹

$$\Delta_{\text{sub}}H = ZRT^2 \frac{d \ln p}{dT} \quad (7)$$

with

$$\ln p = A + \frac{B}{T} + C \ln T + DT^E \quad (8)$$

The values at 700 K are 163 ± 9 kJ mol^{−1} for PRP and 170 ± 12 kJ mol^{−1} for GP. They compare well with the experimental data at about the same temperature, reported in the NIST Database.³² From a direct extrapolation of our results to 298.15 K and 1 bar, we estimated the standard enthalpies of sublimation: 166 ± 9 kJ mol^{−1} for PRP and 173 ± 12 kJ mol^{−1} for GP. However, using the correction from 700 to 298.15 K calculated by Diogo et al.³³ (47.3 kJ mol^{−1}), we estimated standard enthalpies of sublimation for PRP and GP to be, respectively, 210 and 217 kJ mol^{−1}. Both sets of values, though, interpolate the reported experimental standard enthalpies of sublimation³². Moreover, in a very recent review, Markov et al.³⁴ recommends the following experimental values: 181 ± 2 kJ mol^{−1} for the standard enthalpy of sublimation and 175 ± 14 kJ mol^{−1} for the third-law enthalpy. An extrapolation of our results to absolute zero gives 167 kJ mol^{−1} for PRP and 174 kJ mol^{−1} for GP, which within the error, coincide with the experimental value. Also, the value for GP is in excellent agreement with the theoretical result (174.2 kJ mol^{−1}) obtained by Zubov et al.¹⁷ with the same potential.

Although to the best of our knowledge there are no experimental data for the enthalpies of melting and vaporization, we can predict them from the simulated phase diagrams. For example, for GP at 1600 K (near the triple point), we estimate ~ 53 kJ mol^{−1} for the melting enthalpy and ~ 97 kJ mol^{−1} for the vaporization enthalpy. The respective values for PRP at 1700 K (also near the triple point) are ~ 45 and ~ 89 kJ mol^{−1}. The

full analysis of the predicted enthalpies of melting and vaporization will be reported soon.³⁵

The higher enthalpy values for GP reflect that its potential well is narrower and slightly deeper than the PRP well. This is not totally visible in Figure 1 because the plots are in reduced units.

Finally, it is worth mentioning that we have completed³⁶ a systematic study of the enthalpies of sublimation of model C_{n≥70} fullerenes with GP. As a further test of the reliability of our method for the determination of the triple-point properties, the preliminary result for the triple-point temperature of C₇₀ is 1670–1680 K, in excellent agreement with the value (1650 K) recently reported by Abramo et al.²⁷ obtained through a combination of simulation and theory. The estimated standard enthalpy of sublimation is 194.4 kJ mol^{−1}, also in excellent agreement with the available experimental value, 200 ± 6 kJ mol^{−1}.³²

5. Conclusions

From the results and discussion of the last sections, the following general conclusions can be drawn. The GEMC vapor–liquid coexistence curve determined with PRP has an order parameter ($\rho_L - \rho_V$) greater than the one obtained from GP, reflecting the softer nature of PRP. Thus, the critical temperature (2006 ± 27 K) is greater than the temperature estimated with GP (1951 ± 28 K). These values are in good agreement with the ones from other authors.

Two sets of simulations were performed for the fluid–solid coexistence. The results are significantly different. One set was carried out by setting up the starting points in the limit of high temperature. From those points, with decreasing temperature, a series of coexistent states were calculated by GDMC. We found a triple-point temperature of 1858 ± 32 K for PRP and 1898 ± 21 K for GP. According to these results, the stable liquid phase of C₆₀ extends over ~ 150 K for PRP and ~ 50 K for GP. These values agree well with results of other authors that were based on free-energy calculations. Nevertheless, either their results or ours show a liquid phase below the triple points. This may be thermodynamically questionable because the liquid there appears to be stable. However, the fluid–solid relative chemical potentials seem to suggest that this set of simulations corresponds to local minima of the Gibbs free energy.

The origin of this apparently anomalous behavior may presumably be ascribed to the heavy short-range nature of the potential models and to their narrow and deep wells. In the limit of high temperature, the kinetics is violently collisional, and the system eventually approaches hard-sphere behavior. On the contrary, in the limit of low temperature, the system probably samples the narrow and deep potential wells, approaching the usual behavior of attractive potentials.

In the second set of calculations, we decreased the temperature of the Gibbs ensemble vapor–liquid simulations by small steps until a temperature was reached below which the liquid phase is not stable anymore and the system assumed a vapor–solid configuration. From that state, in the limit of low temperature (taken as the triple point), a series of coexistent fluid–solid states were simulated by GDMC by increasing the temperature of the system. From these calculations, we estimated the triple-point temperatures to be 1570 ± 20 K for PRP and 1529 ± 36 K for GP. Below these points, though, a liquid phase is not observed, and from there up, the fluid–solid lines display conventional behavior, in accordance with some theoretical methods and thermodynamics. Moreover, the fluid–solid relative chemical potentials seem to suggest that this set of simulations corresponds to the global minima of the Gibbs free energy. Also, the radial distribution functions and the self-diffusion coefficients inside the liquid pockets, determined from

these triple-points, are consistent with a normal liquid phase, and no sign of liquid supercooling was observed. Therefore, we predict a stable liquid phase, for the PRP model, in the range of temperature 1570 ± 20 K to 2006 ± 27 K. For the GP model, a stable liquid phase between 1529 ± 36 K and 1951 ± 28 K is predicted. Thus, according to these results, the liquid phase of C_{60} extends over almost 450 K, a temperature range considerably wider than the ones found by other authors on the basis of free-energy calculations.

By taking the previous triple points as starting states and successively decreasing the temperature, we simulated the vapor–solid coexistence lines by GDMC. This enabled us to calculate the enthalpies of sublimation as a function of temperature. The values at 700 K are 163 ± 9 kJ mol^{−1} for PRP and 170 ± 12 kJ mol^{−1} for GP, in good agreement with the available experimental results at the same temperature. Additionally, the estimated standard enthalpies of sublimation interpolate the reported experimental values, and the third-law enthalpies are in excellent agreement with experimental and theoretical data. Thus, considering the way the simulations were conducted, that is to say, starting from the triple points determined by our method, we believe that at least the low-temperature triple-point properties should approach those of real C_{60} . We are well aware that some experiments show that solid C_{60} is unstable at ~ 1200 K. Therefore, our conjecture that the low-temperature triple-point properties should approach those of real C_{60} can be confirmed or dismissed only if there are experimental means to prevent the decomposition of fullerite. We have also predicted a few values for the enthalpies of melting and vaporization.

We point out that the present fluid–solid simulations performed by the method of Agrawal and Kofke, from the high-temperature limit, reproduce very well the results reported hitherto from free-energy calculations. The excellent equality of simulated relative chemical potentials of the fluid and solid confirms the consistency of those results. Thus, we believe that both sets of triple-point data are credible as far as the present additive models are concerned. It would be very important to retrace the evolution of the absolute free energy over the entire density and temperature ranges of interest. Would the low-temperature behaviors detected in the present simulations not also turn out? Calculations in this direction are in progress.

On the whole, the differences between the present interaction potentials do not induce significant qualitative changes in the phase behavior of the two models. However, the differences are clearly reflected in the location of the coexistence lines and the values of the critical- and triple-point properties as well as in the enthalpies of sublimation.

Finally, it would be interesting to investigate the role of three-body forces on the PRP model. Some years ago, we showed³⁷ that those forces are of the utmost importance in the vapor–liquid equilibrium of argon. It is expected that they will also induce changes in the critical- and triple-point properties of this C_{60} model. Indeed, because such forces are on average repulsive, the order parameter of the vapor–liquid line will presumably decrease. Thus, it seems that the critical temperature should be lower than the one predicted by the present PRP additive model. Work along these lines is also in progress.

Acknowledgment. We thank Professors J.A. Martinho Simões and M.E. Minas Piedade for providing useful references

and for helpful discussions on the enthalpies of sublimation. Fundação para a Ciência e a Tecnologia (FCT) is gratefully acknowledged for financial support.

References and Notes

- (1) Fartaria, R. P. S.; Fernandes, F. M. S. S.; Freitas, F. F. M.; Rodrigues, P. C. R. *Int. J. Quantum Chem.* **2001**, *84*, 375. Fartaria, R. P. S.; Fernandes, F. M. S. S.; Freitas, F. F. M.; Rodrigues, P. C. R. *Int. J. Quantum Chem.* **2002**, *88*, 355.
- (2) Pacheco, J. M.; Ramalho, J. P. P. *Phys. Rev. Lett.* **1997**, *79*, 3873.
- (3) Hagen, M. H. J.; Meijer, E. J.; Mooij, G. C. A. M.; Frenkel, D.; Lekkerkerker, H. N. W. *Nature (London)* **1993**, *365*, 425.
- (4) Cheng, A.; Klein, M. L.; Caccamo, C. *Phys. Rev. Lett.* **1993**, *71*, 1200.
- (5) Girifalco, L. A. *J. Phys. Chem.* **1991**, *95*, 5370. Girifalco, L. A. *J. Phys. Chem.* **1992**, *96*, 858.
- (6) Tau, M.; Parola, A.; Pini, D.; Reatto, L. *Phys. Rev. E* **1995**, *52*, 2644.
- (7) Broughton, J. Q.; Lill, J. V. *Phys. Rev. B* **1997**, *55*, 2808.
- (8) Ferreira, A. L. C.; Pacheco, J. M.; Prates-Ramalho, J. P. *J. Chem. Phys.* **2000**, *113*, 738.
- (9) Hasegawa, M.; Ohno, K. *J. Chem. Phys.* **1999**, *111*, 5955.
- (10) Hasegawa, M.; Ohno, K. *J. Chem. Phys.* **2000**, *113*, 4315.
- (11) Mederos, L.; Navascués, G. *Phys. Rev. B* **1994**, *50*, 1301.
- (12) Hasegawa, M.; Ohno, K. *Phys. Rev. E* **1996**, *54*, 3928.
- (13) Hasegawa, M.; Ohno, K. *J. Phys.: Condens. Matter* **1997**, *9*, 3361.
- (14) Caccamo, C.; Costa, D.; Fucile, A. *J. Chem. Phys.* **1997**, *106*, 255.
- (15) Caccamo, C. *Phys. Rev. B* **1995**, *51*, 3387.
- (16) Caccamo, C. *Phys. Rep.* **1996**, *274*, 1.
- (17) Zubov, V. I.; Sanches-Ortiz, J. F.; Rabelo, J. N. T.; Zubov, I. V. *Phys. Rev. B* **1997**, *55*, 1.
- (18) Abramo, M. C.; Coppolino, G. *Phys. Rev. B* **1998**, *58*, 2372.
- (19) Panagiotopoulos, A. Z. *Mol. Phys.* **1987**, *61*, 813.
- (20) Panagiotopoulos, A. Z.; Quirke, N.; Stapleton, M.; Tildesley, D. J. *Mol. Phys.* **1988**, *63*, 527.
- (21) Kofke, D. A. *J. Chem. Phys.* **1993**, *98*, 4149.
- (22) Fernandes, F. M. S. S.; Fartaria, R. P. S.; Freitas, F. F. M. *Comput. Phys. Commun.* **2001**, *141*, 403.
- (23) Agrawal, R.; Kofke, D. A. *Mol. Phys.* **1995**, *85*, 23.
- (24) Agrawal, R.; Kofke, D. A. *Mol. Phys.* **1995**, *85*, 43.
- (25) Wang, C. Z.; Xu, C. H.; Chan, C. T.; Ho, K. M. *J. Phys. Chem.* **1992**, *96*, 3563.
- (26) Serra, S.; Sanguinetti, S.; Colombo, L. *J. Chem. Phys.* **1995**, *102*, 2151.
- (27) Abramo, M. C.; Caccamo, C.; Costa, D.; Pellicane, G. *Europhys. Lett.* **2001**, *54*, 468.
- (28) Ashcroft, W. *Nature (London)* **1993**, *365*, 387.
- (29) Stanley, H. E. *Introduction to Phase Transitions and Critical Phenomena*; Oxford University Press: New York, 1971.
- (30) Frenkel, D.; Smit, B. *Understanding Molecular Simulation: From Algorithms to Applications*; Academic Press: San Diego, 1996.
- (31) Diogo, H. P.; Santos, R. C.; Nunes, P. M.; Piedade, M. E. M. *Thermochim. Acta* **1995**, *249*, 113.
- (32) NIST Chemistry WebBook. <http://webbook.nist.gov>; NIST Standard Reference Database Number 69, July 2001; Linstrom, P. J., Mallard, W. G., Eds., National Institute of Standards and Technology: Gaithersburg, MD.
- (33) Diogo, H. P.; Piedade, M. E. M.; Dennis, T. J. S.; Hare, J. P.; Kroto, H. W.; Taylor, R.; Walton, D. R. M. *J. Chem. Soc., Faraday Trans.* **1993**, *89*, 3541.
- (34) Markov, V. Y.; Boltalina, O. V.; Sidorov, L. N. *Russ. J. Phys. Chem.* **2001**, *75*, 1.
- (35) Fernandes, F. M. S. S.; Fartaria, R. P. S.; Freitas, F. F. M. To be submitted for publication.
- (36) Fernandes, F. M. S. S.; Fartaria, R. P. S.; Freitas, F. F. M. To be submitted for publication.
- (37) Rodrigues, S. P. J.; Fernandes, F. M. S. *J. Phys. Chem.* **1994**, *98*, 3917.